

Article

Analysis of Energy Flux Vector on Natural Convection Heat Transfer in Porous Wavy-Wall Square Cavity with Partially-Heated Surface

Yan-Ting Lin ¹ and Ching-Chang Cho ^{2,*}

¹ Institute of Nuclear Energy Research, Atomic Energy Council, Taoyuan 32546, Taiwan; yantinglin@iner.gov.tw

² Department of Vehicle Engineering, National Formosa University, No.64, Wunhua Rd., Huwei Township, Yunlin County 632, Taiwan

* Correspondence: cccho@nfu.edu.tw; Tel.: +886-5-6315699

Received: 16 October 2019; Accepted: 20 November 2019; Published: 22 November 2019



Abstract: The study utilizes the energy-flux-vector method to analyze the heat transfer characteristics of natural convection in a wavy-wall porous square cavity with a partially-heated bottom surface. The effects of the modified Darcy number, modified Rayleigh number, modified Prandtl number, and length of the partially-heated bottom surface on the energy-flux-vector distribution and mean Nusselt number are examined. The results show that when a low modified Darcy number with any value of modified Rayleigh number is given, the recirculation regions are not formed in the energy-flux-vector distribution within the porous cavity. Therefore, a low mean Nusselt number is presented. The recirculation regions do still not form, and thus the mean Nusselt number has a low value when a low modified Darcy number with a high modified Rayleigh number is given. However, when the values of the modified Darcy number and modified Rayleigh number are high, the energy flux vectors generate recirculation regions, and thus a high mean Nusselt number is obtained. In addition, in a convection-dominated region, the mean Nusselt number increases with an increasing modified Prandtl number. Furthermore, as the length of the partially-heated bottom surface lengthens, a higher mean Nusselt number is presented.

Keywords: energy flux vector; porous cavity; natural convection; wavy-wall; heat transfer enhancement; visualization technique

1. Introduction

The plot of the heat flow paths is important since it can provide physical insights into the energy transport process in detail. To achieve this purpose, Kimura and Bejan [1] have suggested a heatline visualization technique. Following the study of Kimura and Bejan [1], numerous researchers have explored the process of heat transport within thermal-fluid systems by utilizing the technique [2–4].

Hooman [5,6] has presented an energy-flux-vector method, which is basically similar to the heatline technique, for visualizing the heat flow paths. Comparing the two visualization methods, Hooman [5,6] has pointed out that the energy-flux-vector method is simpler than the heatline visualization technique since the algebraic equations do not require solving. In the literature, numerous researchers [7–9] have demonstrated that the process of heat transport can be completely explained by using the energy-flux-vector method.

Natural convection in porous cavities has numerous practical applications in engineering fields, including biomedical engineering, chemical and material processing, fluidized beds, geothermal engineering, thermal insulation, solar collection, and so on [10–14]. To achieve the purpose

of heat transfer enhancement, wavy-surface geometries are often imposed [7,8]. Note that the practical applications for the natural convection in a wavy-wall cavity include heat exchangers, solar collectors, condensers in refrigerators, geothermal engineering, and so on [15–17]. In the literature, the investigation into the natural convection heat transfer behavior in a porous cavity with wavy surfaces has been widely discussed [18–20]. The results have demonstrated that the use of the wavy-surface geometries can improve the heat transfer effect. Recently, Biswal et al. [21] have utilized the energy-flux-vector method to explain the process of heat transport of natural convection within a porous cavity with curved side walls. Their results have shown that given suitable curved-side wall forms with appropriate flow conditions, the heat transfer performance can be enhanced.

As discussed above, the analysis of the energy-flux-vector method on natural convection heat transfer in a porous cavity with wavy surfaces has attracted little attention. Accordingly, in the current study, the energy-flux-vector method is utilized to analyze the heat transfer characteristics of natural convection within a porous square cavity bounded by a partially-heated flat bottom wall, low temperature left and right wavy-walls, and an insulated flat top wall. The simulations focus particularly on the effects of the modified Darcy number, modified Rayleigh number, modified Prandtl number, and length of the partially-heated bottom surface on the energy-flux-vector distribution and mean Nusselt number, respectively.

2. Mathematical Formulation

2.1. Governing Equations and Boundary Conditions

Figure 1 illustrates the studied porous square wavy-wall cavity with a partially-heated bottom surface and a characteristic length of L_c . As shown, the partially-heated wall surface has a length of L_H , and it is placed on the center of the bottom wall. Meanwhile, the left and right walls are assumed to have a constant low temperature and a complex-wavy surface.

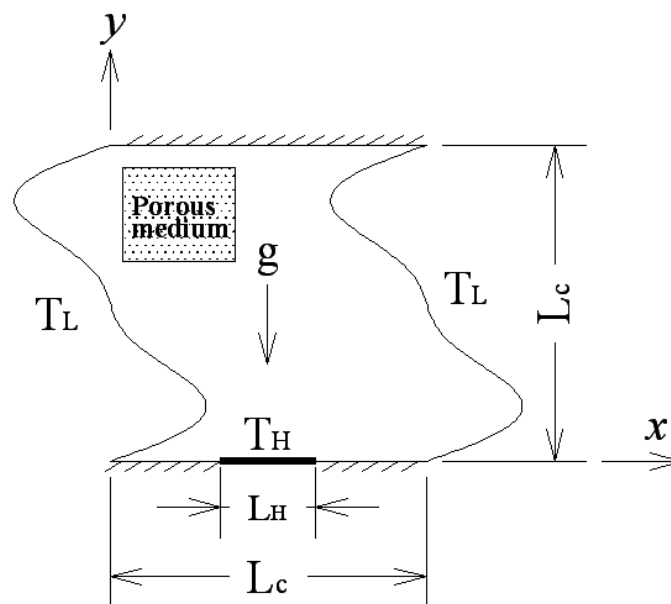


Figure 1. Geometry of partially-heated wavy-wall porous cavity.

It is assumed that the working fluid is Newtonian and incompressible, and the flow and temperature fields are two-dimensional and steady state. In addition, it is also assumed that the Rayleigh number is less than 10^9 and thus, the assumption of laminar flow is valid. Furthermore, the Boussinesq approximation [7,8,22] is imposed, and the local thermal equilibrium condition is assumed to be achieved.

Defining the non-dimensional quantities are as follows [14]:

$$\begin{aligned} x^* &= \frac{x}{L_c}, y^* = \frac{y}{L_c}, \alpha_{eff} = \frac{k_{eff}}{\varepsilon \rho C_p}, u^* = \frac{u L_c}{\alpha_{eff}}, v^* = \frac{v L_c}{\alpha_{eff}}, p^* = \frac{\rho L_c^2}{\rho \alpha_{eff}^2}, \\ \theta &= \frac{T - T_L}{T_H - T_L}, K_m = \frac{K}{\varepsilon}, Pr_m = \frac{\mu}{\rho \alpha_{eff}}, Da_m = \frac{K_m}{L_c^2}, Ra_m = \frac{\rho g \beta L_c^3 (T_H - T_L)}{\mu \alpha_{eff}} \end{aligned} \quad (1)$$

where ρ , C_p , and p represent the density, specific heat, and pressure, respectively; u and v are the velocity components along x - and y -axes, respectively; T_H and T_L signify the high temperature and low temperature, respectively; subscript m indicates the modified value; and superscript $*$ denotes the non-dimensional quantity. After the viscous dissipation and thermal radiation effects are ignored, the continuity, momentum and energy conservation equations described the flow behavior and heat transfer characteristics of natural convection within the porous cavity is written in the following non-dimensionalized forms [14]:

Continuity equation:

$$\frac{\partial u^*}{\partial x^*} + \frac{\partial v^*}{\partial y^*} = 0 \quad (2)$$

x -direction momentum equation:

$$u^* \frac{\partial u^*}{\partial x^*} + v^* \frac{\partial u^*}{\partial y^*} = -\frac{\partial p^*}{\partial x^*} - \frac{Pr_m}{Da_m} u^* + Pr_m \left(\frac{\partial^2 u^*}{\partial x^{*2}} + \frac{\partial^2 u^*}{\partial y^{*2}} \right) - \frac{1.75}{\sqrt{150}} \frac{\sqrt{u^{*2} + v^{*2}}}{\sqrt{Da_m}} u^* \quad (3)$$

y -direction momentum equation:

$$u^* \frac{\partial v^*}{\partial x^*} + v^* \frac{\partial v^*}{\partial y^*} = -\frac{\partial p^*}{\partial y^*} - \frac{Pr_m}{Da_m} v^* + Pr_m \left(\frac{\partial^2 v^*}{\partial x^{*2}} + \frac{\partial^2 v^*}{\partial y^{*2}} \right) - \frac{1.75}{\sqrt{150}} \frac{\sqrt{u^{*2} + v^{*2}}}{\sqrt{Da_m}} v^* + Ra_m \cdot Pr_m \cdot \theta \quad (4)$$

Energy conservation equation:

$$u^* \frac{\partial \theta}{\partial x^*} + v^* \frac{\partial \theta}{\partial y^*} = \frac{\partial^2 \theta}{\partial x^{*2}} + \frac{\partial^2 \theta}{\partial y^{*2}} \quad (5)$$

The dimensionless boundary conditions are expressed as follows:

Bottom partially-heat wall:	$u^* = v^* = 0,$	$\theta = 1$
Bottom other walls:	$u^* = v^* = 0,$	$\partial \theta / \partial \vec{n}^* = 0$
Left and right wavy walls:	$u^* = v^* = 0,$	$\theta = 0$
Top wall:	$u^* = v^* = 0,$	$\partial \theta / \partial \vec{n}^* = 0$

where \vec{n}^* is the normal vector.

2.2. Energy Flux Vectors and Nusselt Number

The energy flux vectors (\vec{E}) are defined as follows [5–9]:

$$\vec{E} = \frac{\partial H^*}{\partial y^*} \vec{i} - \frac{\partial H^*}{\partial x^*} \vec{j} \quad (6)$$

$$\frac{\partial H^*}{\partial y^*} = u^* \theta - \frac{\partial \theta}{\partial x^*}, \quad (7)$$

$$-\frac{\partial H^*}{\partial x^*} = v^* \theta - \frac{\partial \theta}{\partial y^*}. \quad (8)$$

Note that H^* is the non-dimensional heat function, and \vec{i} and \vec{j} are the unit components in x - and y -directions, respectively.

The mean Nusselt number (Nu_m) along the partially-heated bottom surface is defined as follows:

$$Nu_m = \int Nud\xi \quad (9)$$

where $Nu (= \frac{hL_c}{k_{eff}} = -\left(\frac{\partial\theta}{\partial n^*}\right))$ is the Nusselt number, and h is the convection heat transfer coefficient.

2.3. Geometric Description and Numerical Method

In this study, the left and right walls of the porous cavity are assumed to have a complex-wavy surface, which is formulated as follows [7,8]:

$$y^* = \alpha_w \sin(2\pi x^*) + \frac{\alpha_w}{2.5} \sin(4\pi x^*) \quad (10)$$

where α_w is the amplitude of the wavy surface.

In the current study, the generalized coordinate transform technique, finite volume method, and SIMPLE algorithm are used to solve the governing equations presented in Equations (2)–(5). The numerical methods are identical to those used in our previous studies [7,8]. A detailed description of the numerical methods applied in this work can be found in [7,8].

2.4. Numerical Validation and Grid Independence Evaluation

The currently used numerical models and numerical methods were valid by comparing the current results with those presented by Singh et al. [14]. Table 1 shows these results. Note that the Rayleigh number of $Ra = 10^5$, porosity of $\varepsilon = 0.6$, and Prandtl number of $Pr = 1$ are given in the case. It is shown that the current results are identical to those presented in Singh et al. [14].

Table 1. Comparison of current results for mean Nusselt number with Singh et al. [14] for two different Darcy numbers.

	$Da = 10^{-2}$	$Da = 10^{-4}$
Current results	3.441	1.067
Singh et al. [14]	3.461	1.067
Error (%)	0.6	0.0

The mesh sizes of 101×201 , 101×501 , 101×1001 , 201×1001 have been examined for the variation of mean Nusselt number, respectively, and the results showed that the mesh size of 101×1001 has a grid-independent solution.

3. Results and Discussion

In the study, the ranges of the non-dimensional parameters were set as follows: modified Darcy number: $Da_m = 10^{-5}$ to $Da_m = 10^{-2}$; modified Rayleigh number: $Ra_m = 10^2$ to $Ra_m = 10^5$; modified Prandtl number: $Pr_m = 0.1$ to $Pr_m = 10$; amplitude of wavy surface: $\alpha_w = 0.25$; and length of the partially-heated bottom surface: $L_H^* = 0.3$ to $L_H^* = 0.9$.

Figures 2 and 3 illustrate the distributions of the energy flux vectors and isotherms within the porous cavity for various modified Darcy numbers and modified Rayleigh numbers. Figure 4 shows the effects of the modified Darcy number and modified Rayleigh number on the mean Nusselt number. According to the definition of the energy flux vectors given in Equation (6), the conduction mechanism dominates if the flow of energy flux vectors is directly from the bottom partially-heated high-temperature wall to the left and right low-temperature wavy-walls, while the convection mechanism dominates if the energy flux vectors generate closed recirculation regions [5–9]. Therefore, as shown in Figure 2a, when the values of the modified Darcy number and modified Rayleigh number are both low, the heat transfer effect within the porous partially-heated cavity is dominated by a pure

conduction mechanism since the closed recirculation regions in the energy-flux-vector distribution are not created. In addition, a low modified Darcy number represents a low permeability due to the presence of a high flow resistance [14]. Therefore, although a larger buoyancy effect induced by giving a high modified Rayleigh number is presented, a high flow resistance is also generated within the porous partially-heated cavity. As a result, the energy flux vectors do still not form closed recirculation regions, and thus the conduction mechanism continually dominates heat transfer behavior (see Figure 2b). Under conduction-dominance, the high-temperature fluid heated by the partially-heated bottom surface is slowly diffused to left and right low-temperature wavy-wall surfaces to be dissipated (see the isotherms in Figure 2). Consequently, under a low modified Darcy number, a low mean Nusselt number is presented, irrespective of the value assigned to the modified Rayleigh number (see Figure 4).

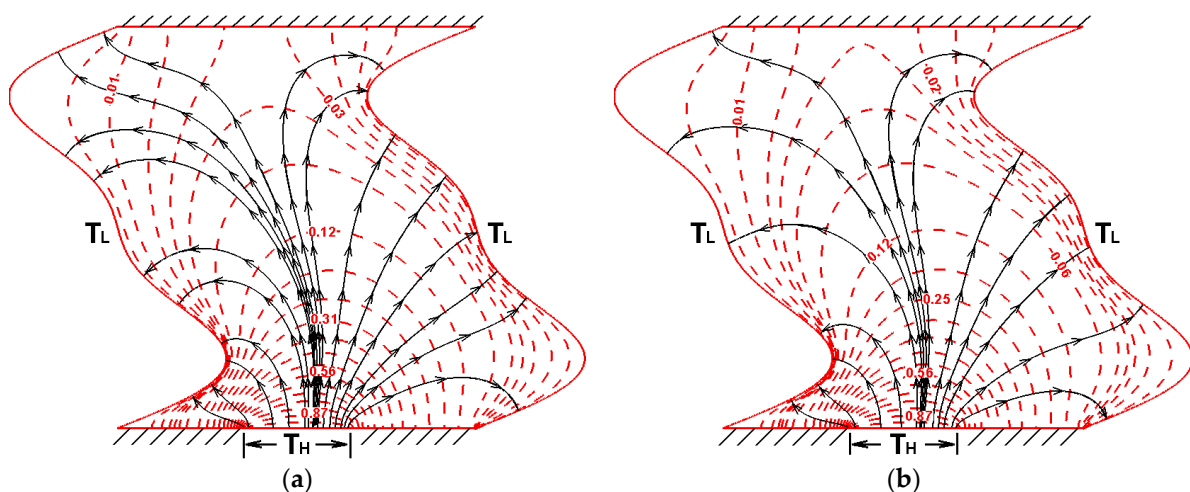


Figure 2. Distributions of energy flux vectors and isotherms within a partially-heated porous cavity given a modified Darcy number of $Da_m = 10^{-5}$ and modified Rayleigh numbers of: (a) $Ra_m = 10^2$ and (b) $Ra_m = 10^5$. Note that $Pr_m = 1$ and $L_H^* = 0.3$. Note also that the black solid lines indicate the flow direction of the energy-flux-vector, while the red dashed lines indicate the isothermal contours.

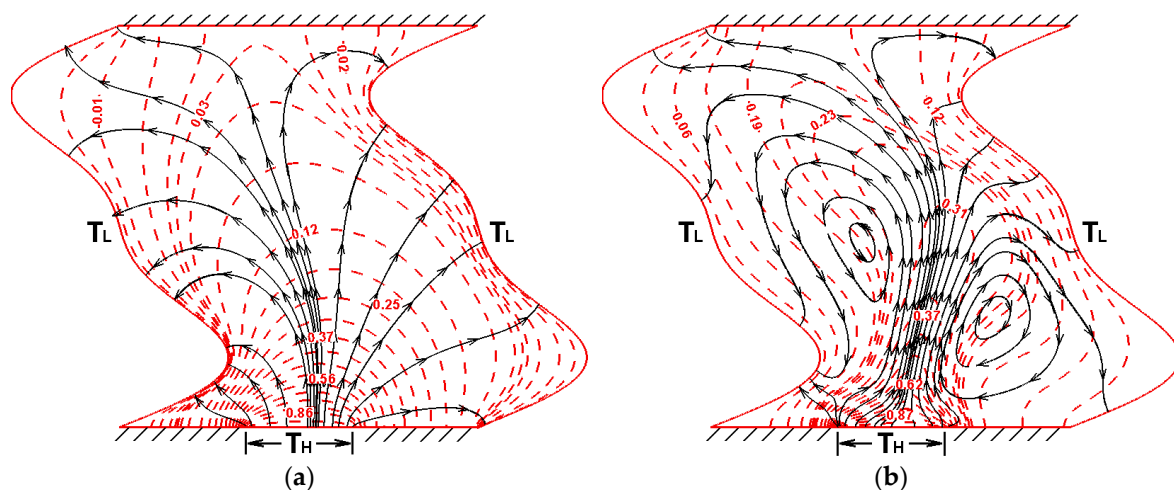


Figure 3. Distributions of energy flux vectors and isotherms within a partially-heated porous cavity given a modified Darcy number of $Da_m = 10^{-2}$ and modified Rayleigh numbers of: (a) $Ra_m = 10^2$ and (b) $Ra_m = 10^5$. Note that $Pr_m = 1$ and $L_H^* = 0.3$. Note also that the black solid lines indicate the flow direction of the energy-flux-vector, while the red dashed lines indicate the isothermal contours.

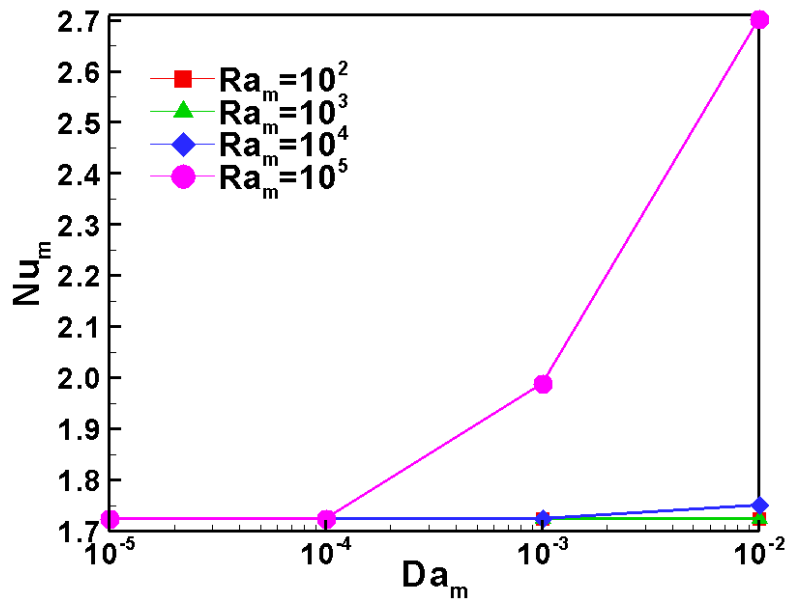


Figure 4. Variation of mean Nusselt number with modified Darcy number as a function of modified Rayleigh number. Note that $Pr_m = 1$ and $L_H^* = 0.3$.

When a high modified Darcy number and a low modified Rayleigh number is given, the closed recirculation regions of the energy flux vectors are still not formed within the porous partially-heated cavity (see Figure 3a). Although a high modified Darcy number has a high permeability and a low flow resistance, a low modified Rayleigh number induces a small buoyancy effect. Therefore, the convection effect is still weak, and the conduction mechanism continues to dominate the heat transfer effect. As a result, a low mean Nusselt number is presented (see Figure 4).

When the modified Darcy number and the modified Rayleigh number are both high, a low flow resistance and a high buoyancy effect occur within the porous partially-heated cavity. Therefore, the closed energy-flux-vector recirculations are formed, resulting in enhancement of the convection effect (see Figure 3b). The high-temperature fluid on the partially-heated bottom wall is promptly driven to the left and right low-temperature walls to be dissipated (see the isotherms in Figure 3b). As a result, a high mean Nusselt number is obtained (see Figure 4).

Figures 5 and 6 illustrate the distributions of the energy flux vectors and isotherms within the porous partially-heated cavity for various modified Prandtl numbers and modified Rayleigh numbers. Figure 7 shows the effects of the modified Prandtl number and modified Rayleigh number on the mean Nusselt number. Note that the modified Darcy number is set as $Da_m = 10^{-2}$ in the cases. It shows that given a low modified Rayleigh number, the distributions of the energy flux vectors and isotherms are similar for various modified Prandtl numbers (see Figure 5a,b). The recirculation regions of energy flux vectors are not created, and thus the conduction heat transfer dominates. In other words, the effect of the modified Prandtl number on the heat transfer is insignificant. Therefore, a low and approximately constant mean Nusselt number is presented (see Figure 7). When a high modified Rayleigh number is given, it shows that the size of closed energy-flux-vector recirculation regions enlarges as the modified Prandtl number is increased (see Figure 6a,b). In other words, a higher modified Prandtl number has a stronger convection effect under high modified Rayleigh numbers. Consequently, a higher mean Nusselt number is presented (see Figure 7).

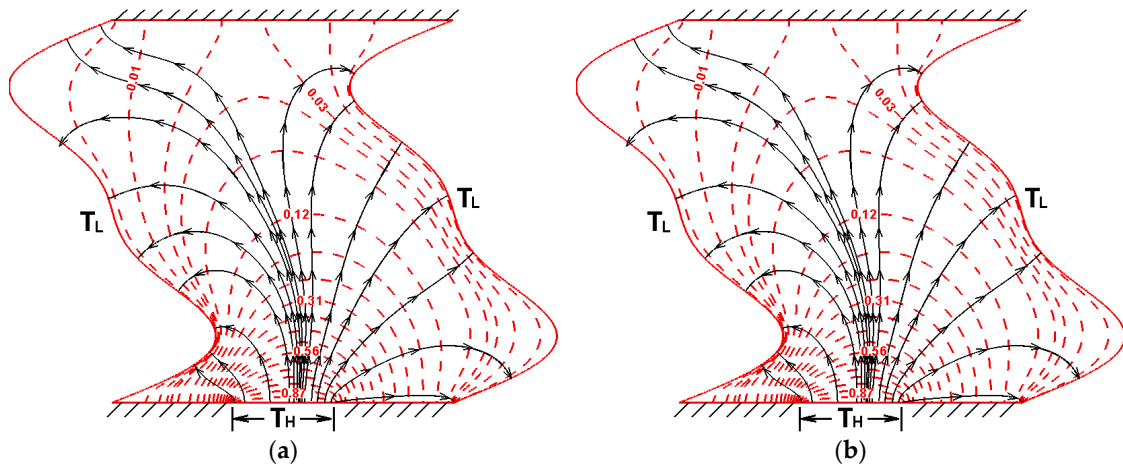


Figure 5. Distributions of energy flux vectors and isotherms within a partially-heated porous cavity given a modified Rayleigh number of $Ra_m = 10^2$ and modified Prandtl numbers of: (a) $Pr_m = 0.1$ and (b) $Pr_m = 10$. Note that $Da_m = 10^{-2}$ and $L_H^* = 0.3$. Note also that the black solid lines indicate the flow direction of energy flux vectors, while the red dashed lines indicate the isothermal contours.

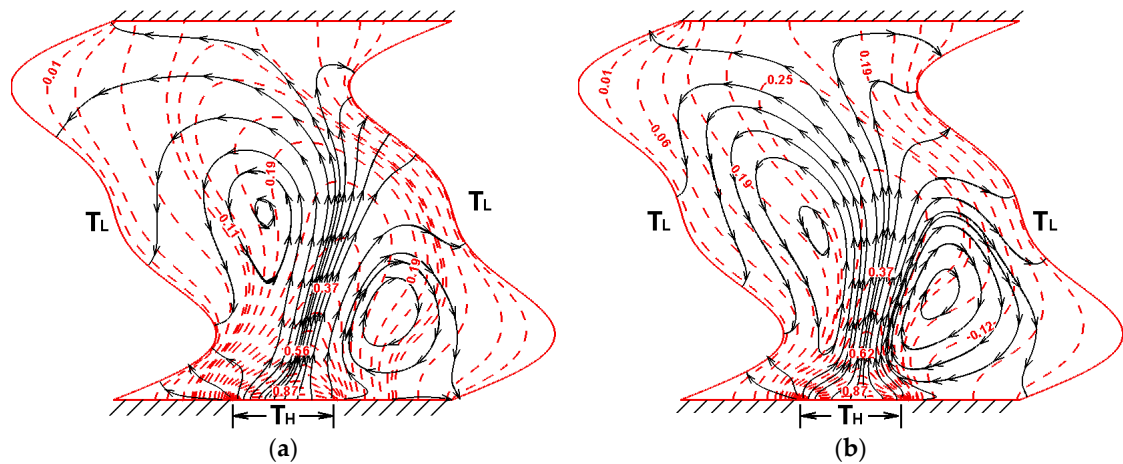


Figure 6. Distributions of energy flux vectors and isotherms within a partially-heated porous cavity given a modified Rayleigh number of $Ra_m = 10^5$ and modified Prandtl numbers of: (a) $Pr_m = 0.1$ and (b) $Pr_m = 10$. Note that $Da_m = 10^{-2}$ and $L_H^* = 0.3$. Note also that the black solid lines indicate the flow direction of energy flux vectors, while the red dashed lines indicate the isothermal contours.

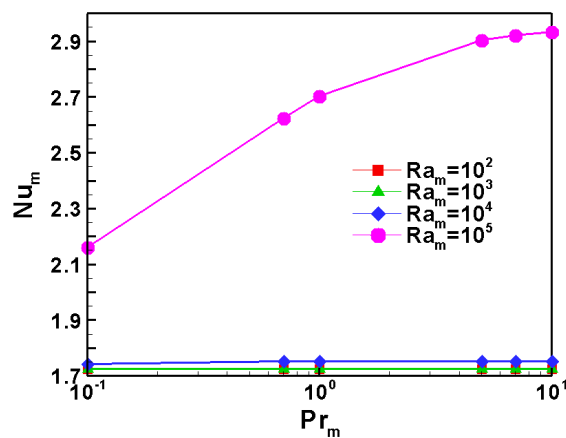


Figure 7. Variation of mean Nusselt number with modified Prandtl number as a function of a modified Rayleigh number. Note that $Da_m = 10^{-2}$ and $L_H^* = 0.3$.

Figure 8 illustrates the distributions of the energy flux vectors within the porous cavity for various partially-heated lengths and modified Rayleigh numbers. Figure 9 shows the effects of the partially-heated length and modified Rayleigh number on the mean Nusselt number. Note that the modified Darcy number is set as $Da_m = 10^{-2}$ in these cases. For a low modified Rayleigh number, the conduction heat transfer dominates since the recirculation regions of the energy flux vectors are not formed within the porous cavity for various partially-heated lengths (see Figure 8a). Therefore, a low mean Nusselt number is presented. As the length of the partially-heated bottom surface is lengthened, a larger bottom heated area is presented. Consequently, a higher mean Nusselt number is obtained (see Figure 9). Given a high modified Rayleigh number, the energy flux vectors form closed recirculation regions. The size of the recirculation regions enlarges as the partially-heated length is extended (see Figure 8b). As a result, the strength of the convection effect enhances. Consequently, the mean Nusselt number rises with the increasing length of the partially-heated bottom surface (see Figure 9).

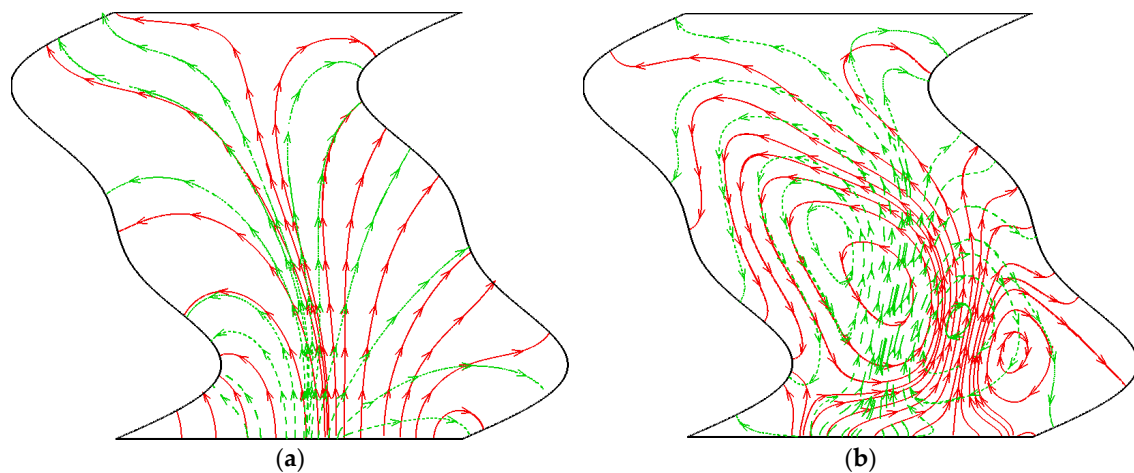


Figure 8. Distributions of energy flux vectors within a porous cavity given partially-heated lengths of $L_H^* = 0.3$ and $L_H^* = 0.9$ and modified Rayleigh numbers of: (a) $Ra_m = 10^2$ and (b) $Ra_m = 10^5$. Note that $Da_m = 10^{-2}$ and $Pr_m = 1$. Note also that the red solid lines indicate the partially-heated length of $L_H^* = 0.9$, and the green dashed lines indicate the partially-heated length of $L_H^* = 0.3$.

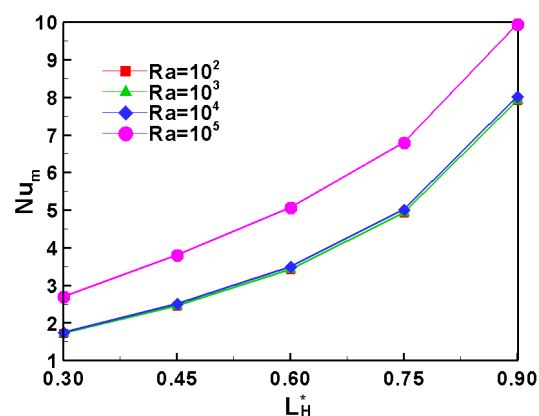


Figure 9. Variation of mean Nusselt number with partially-heated length as a function of a modified Rayleigh number. Note that $Da_m = 10^{-2}$ and $Pr_m = 1$.

4. Conclusions

This paper has analyzed the heat transfer behavior of natural convection in a porous square wavy-wall cavity with a partially-heated bottom surface using the energy-flux-vector method. The effects of the flow parameters and length of a partially-heated bottom surface on the energy-flux-vector distribution and mean Nusselt number have been discussed. The studied results are summarized as follows:

1. Given a low modified Darcy number, the energy flux vectors did not generate recirculation regions within the porous cavity, irrespective of the value assigned to the modified Rayleigh number. The conduction heat transfer dominated, and thus the mean Nusselt number was low.
2. Given a high modified Darcy number and a low modified Rayleigh number, the heat transfer effect was dominated by the conduction mechanism since no recirculation region was formed in the energy flux vectors. Therefore, a low mean Nusselt number was obtained.
3. Given a high modified Darcy number with a high modified Rayleigh number, recirculation regions in the energy-flux-vector distribution were produced, resulting in a convection-domination. Consequently, a high mean Nusselt number was presented.
4. In conduction-dominated region, the effect of the modified Prandtl number on the energy-flux-vector distribution and mean Nusselt number was insignificant. However, in convection-dominated region, the size of the closed energy-flux-vector recirculation region enlarged, and the value of the mean Nusselt number raised as the modified Prandtl number was increased.
5. In conduction-dominated or convection-dominated regions, the mean Nusselt number was raised as the length of the partially-heated bottom surface lengthened.

Author Contributions: Conceptualization, C.-C.C.; Methodology, C.-C.C.; Software, C.-C.C. and Y.-T.L.; Validation, C.-C.C. and Y.-T.L.; Formal Analysis, C.-C.C.; Investigation, C.-C.C.; Resources, C.-C.C. and Y.-T.L.; Data Curation, C.-C.C. and Y.-T.L.; Writing-Original Draft Preparation, C.-C.C.; Writing-Review & Editing, C.-C.C.; Visualization, C.-C.C.; Supervision, C.-C.C.; Project Administration, C.-C.C.; Funding Acquisition, C.-C.C. and Y.-T.L.

Funding: The authors would like to thank the Ministry of Science and Technology, Taiwan, for the financial support of this study under Contract Nos. MOST 108-2221-E-150-011, MOST 108-3116-F-042A-006 and MOST 107-2221-E-150-035.

Conflicts of Interest: The authors declare no conflict of interest.

Nomenclature

Da_m	modified Darcy number, $Da_m = \frac{K_m}{L_c^2}$
\vec{E}	energy flux vector
k_{eff}	effective thermal conductivity, $Wm^{-1}K^{-1}$
L_c	characteristic length of square cavity, m
L_H	length of partially-heated bottom surface, m
Nu	Nusselt number, $Nu = \frac{hL_c}{k_{eff}} = -\left(\frac{\partial\theta}{\partial n}\right)$
Nu_m	mean Nusselt number, $Nu_m = \int Nud\xi$
Pr_m	modified Prandtl number, $Pr_m = \frac{\mu}{\rho\alpha_{eff}}$
Ra_m	modified Rayleigh number, $Ra_m = \frac{\rho g \beta L_c^3 (T_H - T_L)}{\mu \alpha_{eff}}$
T	temperature, K

Greek symbols

α_{eff}	effective thermal diffusivity, m^2s^{-1}
α_w	amplitude of wavy surface
β	thermal expansion coefficient, K^{-1}
ε	porosity
K	permeability, m^2
θ	dimensionless temperature, $\theta = \frac{T - T_L}{T_H - T_L}$

References

1. Kimura, S.; Bejan, A. The "Heatline" visualization of convective heat transfer. *J. Heat Transf.-Trans. ASME* **1983**, *105*, 916–919. [[CrossRef](#)]
2. Trevisan, O.V.; Bejan, A. Combined heat and mass transfer by natural convection in a vertical enclosure. *J. Heat Transf.-Trans. ASME* **1984**, *109*, 104–112. [[CrossRef](#)]

3. Ramakrishna, D.; Basak, T.; Roy, S.; Pop, I. A complete heatline analysis on mixed convection within a square cavity: Effects of thermal boundary conditions via thermal aspect ratio. *Int. J. Therm. Sci.* **2012**, *57*, 98–111. [[CrossRef](#)]
4. Biswal, P.; Nag, A.; Basak, T. Analysis of thermal management during natural convection within porous tilted square cavities via heatline and entropy generation. *Int. J. Mech. Sci.* **2016**, *115–116*, 596–615. [[CrossRef](#)]
5. Hooman, K.; Gurgenci, H.; Dincer, I. Heatline and energy-flux-vector visualization of natural convection in a porous cavity occupied by a fluid with temperature-dependent viscosity. *J. Porous Media* **2009**, *12*, 265–275. [[CrossRef](#)]
6. Hooman, H. Energy flux vectors as a new tool for convection visualization. *Int. J. Numer. Methods Heat Fluid Flow* **2010**, *20*, 240–249. [[CrossRef](#)]
7. Cho, C.C. Heat transfer and entropy generation of mixed convection flow in Cu-water nanofluid-filled lid-driven cavity with wavy surface. *Int. J. Heat Mass Transf.* **2018**, *119*, 163–174. [[CrossRef](#)]
8. Cho, C.C. Mixed convection heat transfer and entropy generation of Cu-water nanofluid in wavy-wall lid-driven cavity in presence of inclined magnetic field. *Int. J. Mech. Sci.* **2019**, *151*, 703–714. [[CrossRef](#)]
9. Nayak, R.K.; Bhattacharyya, S.; Pop, I. Numerical study on mixed convection and entropy generation of a nanofluid in a lid-driven square enclosure. *J. Heat Transf.-Trans. ASME* **2016**, *138*, 012503. [[CrossRef](#)]
10. Lu, D.A.; Flamant, G.; Snabre, P. Towards a generalized model for vertical walls to gas-solid fluidized beds heat transfer-I. Particle convection and gas convection. *Chem. Eng. Sci.* **1993**, *48*, 2479–2492. [[CrossRef](#)]
11. Nield, D.A.; Bejan, A. *Convection in Porous Media*; Springer: New York, NY, USA, 2006.
12. Prud'homme, M.; Jasmin, S. Inverse solution for a biochemical heat source in a porous medium in the presence of natural convection. *Chem. Eng. Sci.* **2006**, *61*, 1667–1675. [[CrossRef](#)]
13. Al-Amiri, A.; Khanafer, K.; Pop, I. Steady-state conjugate natural convection in a fluid-saturated porous cavity. *Int. J. Heat Mass Transf.* **2008**, *51*, 4260–4275. [[CrossRef](#)]
14. Singh, A.K.; Basak, T.; Nag, A.; Roy, S. Heatlines and thermal management analysis for natural convection within inclined porous square cavities. *Int. J. Heat Mass Transf.* **2015**, *87*, 583–597. [[CrossRef](#)]
15. Misirlioglu, A.; Baytas, A.C.; Pop, I. Free convection in a wavy cavity filled with a porous medium. *Int. J. Heat Mass Transf.* **2005**, *48*, 1840–1850. [[CrossRef](#)]
16. Sultana, Z.; Hyder, M.N. Non-darcy free convection inside a wavy enclosure. *Int. Commun. Heat Mass Transf.* **2007**, *34*, 136–146. [[CrossRef](#)]
17. Cho, C.C.; Chiu, C.H.; Lai, C.Y. Natural convection and entropy generation of Al₂O₃-water nanofluid in an inclined wavy-wall cavity. *Int. J. Heat Mass Transf.* **2016**, *97*, 511–520. [[CrossRef](#)]
18. Kumar, B.V.R.; Singh, P.; Murthy, P.V.S.N. Effect of surface undulations on natural convection in a porous square cavity. *J. Heat Transf.-Trans. ASME* **1997**, *119*, 848–851. [[CrossRef](#)]
19. Chen, X.B.; Yu, P.; Winoto, S.H.; Low, H.T. Free convection in a porous wavy cavity based on the Darcy-Brinkman-Forchheimer extended model. *Numer. Heat Transf. A-Appl.* **2007**, *52*, 377–397. [[CrossRef](#)]
20. Khanafer, K.; Al-Azmi, B.; Marafie, A.; Pop, I. Non-Darcian effects on natural convection heat transfer in a wavy porous enclosure. *Int. J. Heat Mass Transf.* **2009**, *52*, 1887–1896. [[CrossRef](#)]
21. Biswal, P.; Basak, T. Heatlines visualization of convective heat flow during differential heating of porous enclosures with concave/convex side walls. *Int. J. Numer. Methods Heat Fluid Flow* **2018**, *28*, 1506–1538. [[CrossRef](#)]
22. Singh, A.K.; Basak, T.; Nag, A.; Roy, S. Role of entropy generation on thermal management during natural convection in tilted porous square cavities. *J. Taiwan Inst. Chem. Eng.* **2015**, *50*, 153–172. [[CrossRef](#)]

